Improvements to Thermal Protection System Design of Aerocapture Systems for Uranus Orbiters

Jonathan Morgan*
NASA Ames Research Center, Moffett Field, CA, 94035

Joseph Williams†
Analytical Mechanics Associates, INC., Hampton, VA, 23666

The National Academies' Planetary Science and Astrobiology Decadal Survey identified Uranus and Neptune, known as the Ice Giants, as priority destinations for scientific exploration. The survey assessed both the Uranus Orbiter and Probe (UOP) concept for Uranus and the Neptune-Triton Odyssey concept for Neptune, determining that Uranus is the highest priority for a Flagship class mission. The UOP mission concept plans to deliver an in situ probe and conduct a multi-year orbital tour of Uranus to meet the science objectives. While the Uranus mission is currently viable with launch windows starting in 2031 using existing launch vehicles, it has a cruise phase of at least 12 years and would require more than half of its weight in fuel propellant to achieve the necessary velocity change for orbital insertion. Aerocapture uses aerodynamic forces generated by a planet's atmosphere to modulate a spacecraft's trajectory, decreasing its velocity, and allowing mission designers to target the final orbital state. Aerocapture reduces the time of flight from Earth to Uranus compared to a fully propulsive solution, opening up more launch opportunities to achieve the mission's science objectives by the 2040s. Aerocapture also allows for an increase in payload mass by mitigating the need for fuel to retropropulsively insert the payload into orbit, thereby enabling more scientific research. For an aerocapture mission structure using a traditional aeroshell to deliver the UOP's scientific payload to Uranus, Conformal Phenolic Impregnated Carbon Ablator (C-PICA) was determined to be the best-performing forebody thermal protection system (TPS), with other candidate aftbody TPS options also presented as feasible. This paper focuses on: A) evaluating C-PICA as a forebody TPS under stressing entry conditions associated with a wide range of potential Uranus flagship launch vehicles and interplanetary trajectories; B) exploring mass-efficient and cost-efficient aftbody TPS candidates; and C) providing a summary list of actions remaining to ensure a technically feasible and supply-robust set of TPS for an aerocapture vehicle to the Ice Giants.

I. Nomenclature

q_{conv}	=	convective heat flux, W/cm^2
q_{rad}	=	radiative heat flux, W/cm^2
T	=	thickness, cm
V_∞	=	change in velocity, km/s
σ	=	standard deviation
μ	=	mean value

subscripts

1	=	nominal branch
2	=	aerothermal branch
3	=	material branch
RSS	=	Root-Sum-Squared result

*Aerospace Engineer, AIAA Member.

†Aerospace Engineer associated with NASA Ames Research Center, AIAA Member

II. Introduction

The National Academy of Sciences (NAS), from which NASA draws recommendation in selecting future mission proposals, has determined the outer planets Uranus and Neptune - the Ice Giants - are the priority for the next decade of scientific research because of their unique structure and place in our solar system [1]. Work by numerous groups has outlined the feasibility for concept missions to deliver scientific payload both to Neptune's moon Triton and Uranus[2, 3]. As studied in the proposal selected by the NAS, a fully-propulsive vehicle delivery to Uranus may take approximately 13 years, with nearly 50% of the mass devoted to the necessary fuel for propulsive orbital insertion[1]. The large amount of fuel required for this mission severely constrains the available payload for scientific instruments, thereby limiting the quantity of gathered data. Aerocapture, shown conceptually in Fig.1, may drastically reduce both the time and fuel mass required for orbital insertion by making use of the planet's atmosphere to slow down rather than retropropulson. This orbital transfer maneuver can be accomplished in a variety of ways, most simply by Bank Angle Modulation (BAM) as has been used for direct entry on Apollo, Mars Science Laboratory (MSL), Mars2020, and Orion, or by more sophisticated methods of Direct Force Control or Drag Modulated Aerocapture. The most recent study by [4] and others evaluated the feasibility of using a heritage aeroshell design from Mars2020 with BAM aerodynamic control to deliver the conceptual payload from the UOP mission selected by NAS. This paper is an update to previously published work [5] performed during early design and analysis cycles. As such, the background and overview of the aerocapture concept, con-ops, are not covered here. Instead, this work reports updates reflecting the final aeroshell design and analysis cycles, including select trade studies for arrival velocities, aeroshell separation timing, and aftbody thermal protection schemes. A layout of proposed work to ensure that thermal protection systems are sufficiently matured to meet the needs of an aerocapture system that travels to the Ice Giant, Uranus, is also reported. A brief re-cap of the state of the aeroshell design is presented in Section III. Section IV contains analysis of the forebody TPS and trade-space for the backshell heatshields, and their implementation on the vehicles. The mission trade studies and their impact on the TPS are documented in Section V. Section VI contains the updated trade considerations for the aftbody TPS along with their implementation scheme. Future work and a brief high-level assessment of work to go for TPS to mature readiness for an Ice Giants aerocapture mission are presented in Section VIII. Finally, conclusions and forward work for the study are summarized in Section IX.

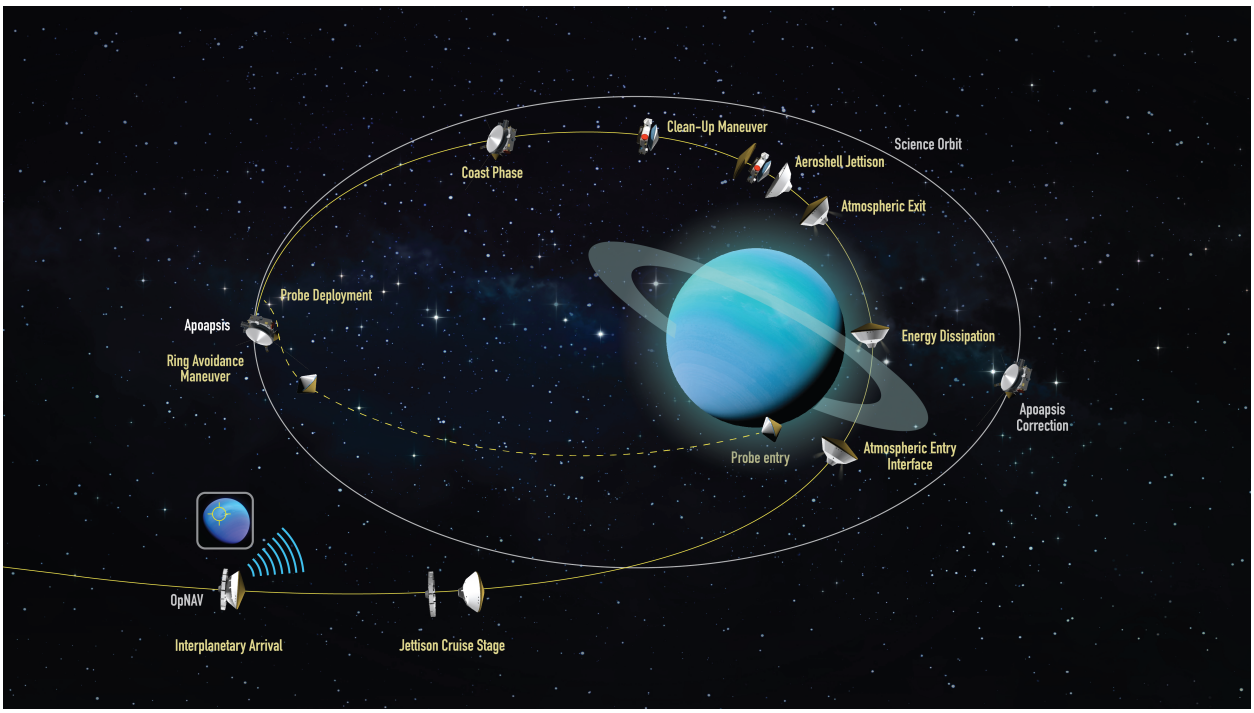

Fig. 1 Conceptual operations for an aerocapture approach to Uranus.

III. Background

In previous work, the aeroshell design was chosen to be an MSL vehicle scaled to a diameter of 5 m. In the latest design analysis cycle (DAC5), shown in Fig.2, the vehicle was modified to be 4.57 m to ensure fitment into the baseline Falcon Heavy Launch vehicle[6]. Adjustments to the aftbody shape were then made to optimize fitment around the antenna and reduce contact with wake flow. The aeroshell's entry corridor into the Uranian Hydrogen and Helium dominated atmosphere is characteristically bounded by "Lift-Up" and "Lift-Down" trajectories. For both trajectories, the aeroshell trims at a constant angle of attack of 17°. Pointing the lift vector toward Uranus produces the lowest heat flux and greatest heat load, defining the Lift-Down trajectory. Alternatively, pointing the lift vector away from the planet produces a design heat flux and the lowest heat load defining the Lift-Up trajectory. The Lift-Up and Lift-down trajectories are intended to envelope the expected detailed design trajectories. Trajectories are constructed using POST2 [7] informed by aerodynamic data from a database produced by [8], and then 3D CFD calculations using LAURA/HARA generate the resultant aerothermal environments [9]. Discrete predictions of surface environments in Fig. 3 show convective heating that is greater than missions like MSL and Mars2020 have experienced, but there is minimal radiative heating, pressure and shear environments predicted, owing to the low density of the upper atmosphere and gas species present. The aerothermal entry environments from LAURA/HARA are then mapped to a series of discrete body points that are distributed across a symmetry plane of the vehicle, described in Fig.4. It is noted that radiative heat flux drops off entirely at approximately 300 *seconds* into the heat pulse , which is due to a numerical switch in LAURA/HARA predictions that discounts radiative heating in latter portions of the trajectory. This is deemed acceptable because the radiative heat flux is minimal in latter portions of the trajectory and is less than 10% of the total heat flux at its maximum. Even more different is long duration of the heat pulse, resulting in a large heat load, laid out in Table 2, from which the TPS must insulate the vehicle. The predicted heat load is reduced by approximately 15% from DAC3 to DAC5, as evidenced by the comparison between DAC3 and DAC5 BP0 predicted heat loads. After the vehicle exits the atmosphere, the scientific payload no longer needs protection and the aeroshell is separated from the orbiter.

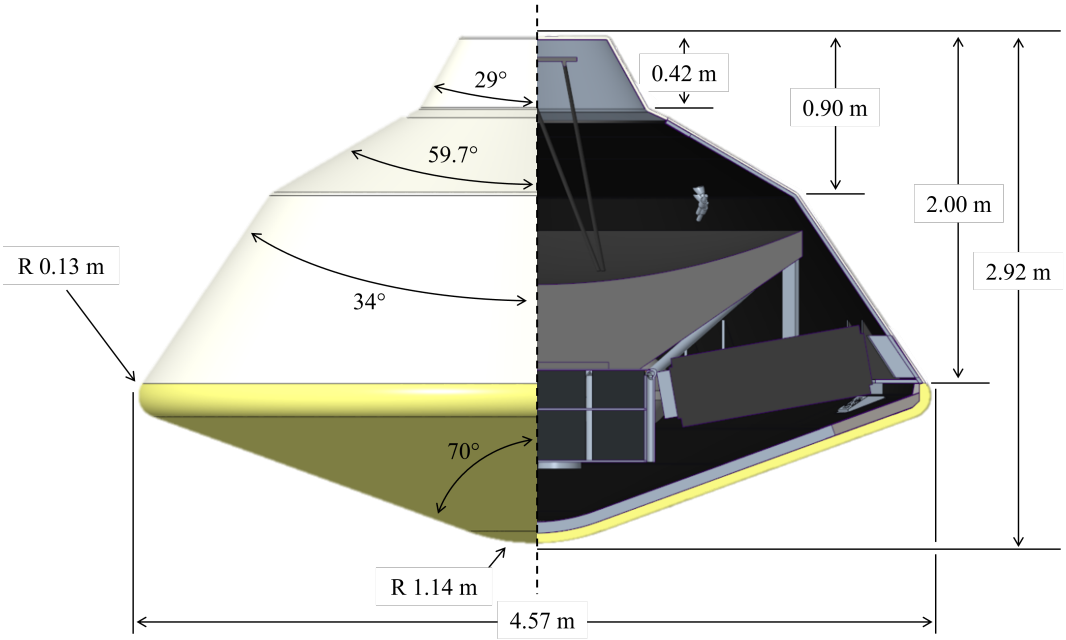

Fig. 2 Aeroshell dimensions and cutaway to internal layout of payload and radioisotope thermal generators.

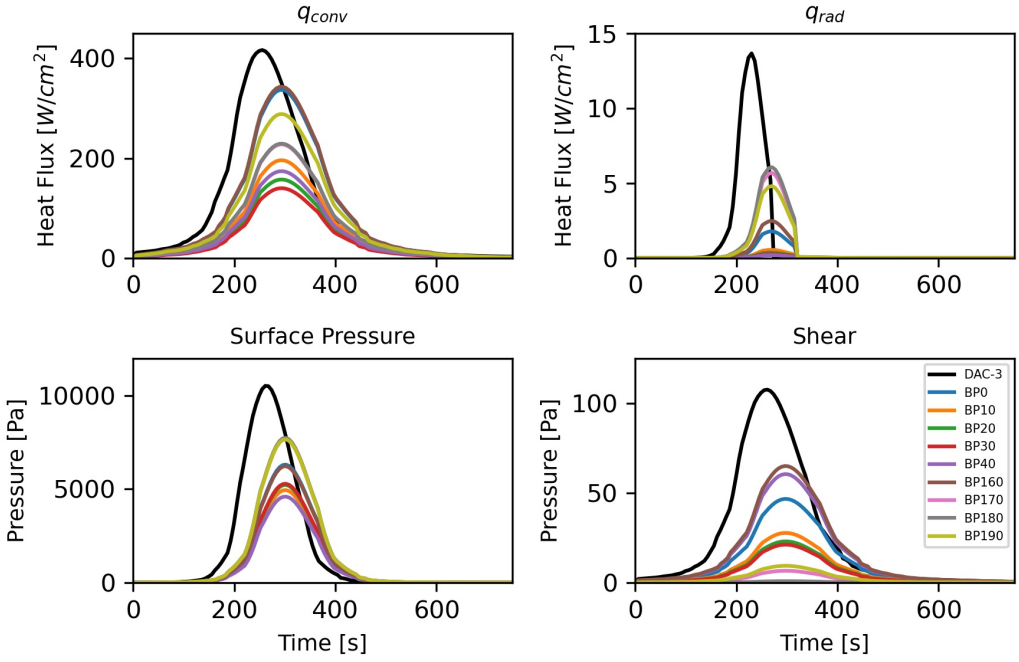

(a) Lift-Up environments

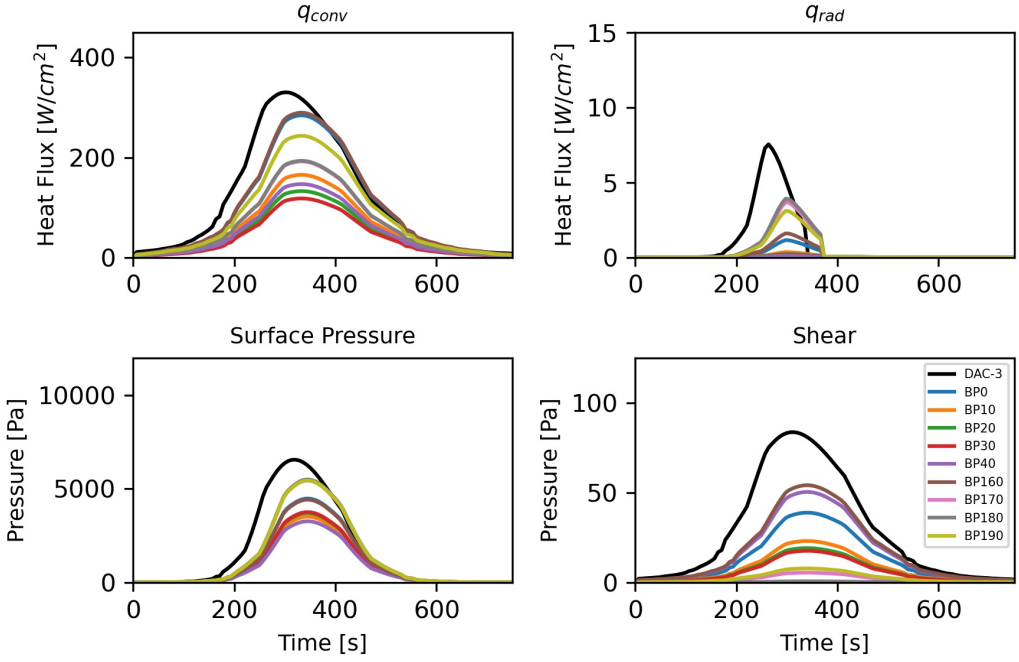

(b) Lift-Down environments

Fig. 3 Plot of a) Convective hot-wall heat flux (q_{conv}), b) radiative hot-wall heat flux (q_{rad}), c) surface normal pressure, d) shear stress for select body points on the forebody.

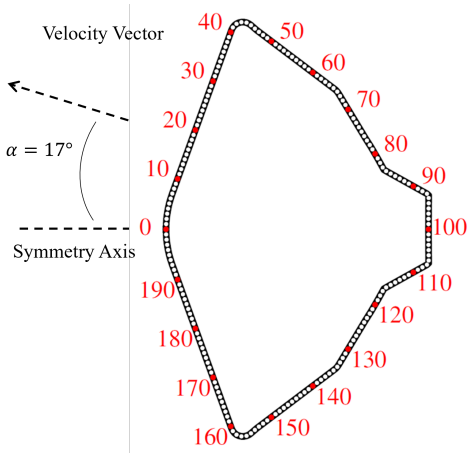

Fig. 4 Body point (BP) mapping around aeroshell.

Design and Analysis Cycle (DAC#)	DAC 3	DAC 5								
Body Point (BP)	0	0	10	20	30	40	160	170	180	190
Lift-Up	72	64	37	30	26	33	66	43	44	55
Lift-Down	87	74	43	34	30	38	75	50	50	63

Table 2 Total heat load (kJ/cm^2) of the Lift-Up and Lift-Down trajectory on each forebody body point.

IV. Forebody TPS Analysis

A. TPS and Assumptions

The sizing methodology for the TPS on the forebody is the same as previous analysis cycles, discussed in detail in Morgan et al.[5]. Simulations show that transition to turbulent flow is possible along the leeward flank but augmentation due to turbulent heating does not exceed the laminar heating on the windward side. Since the vehicle is sized to a constant thickness everywhere, the laminar windside heating profile is then the driving environment for determining TPS thickness on the forebody. In the previous paper, a tiled C-PICA with RTV-560 gap-filler system was analyzed along side tiled PICA-D and 3MDCP as forebody TPS candidates. C-PICA was baselined as the forebody TPS due to mass efficiency and being compliant, a manufacturing advantage that improves performance at the shoulder, where heating and surface shear stress are high. Tiled C-PICA also passes base requirements of showing favorable performance at relevant heat fluxes. Arc jet testing of the candidate TPS is currently limited to heating in air or nitrogen rather than Hydrogen and Helium. As of the publication of this work, tiled C-PICA has been up to 600 W/cm^2 and performed well[10]. As of February 2024, tiled C-PICA has also flown as the forebody TPS for the VARDA Winnebago-1 vehicle, successfully returning to Earth, though at heat rates lower than those being considered in this study[11]. In this work, tiled C-PICA is still the baseline TPS, however, updates to the sizing for the latest nominal trajectories are performed along with updated assumptions in the entry problem formulation. The two adjusted assumptions pertain to the vehicle substructure. The vehicle structure was changed to match the Mars Science Laboratory and Mars 2020 missions, particularly the aluminum honeycomb thickness which changed from 5.84 cm to 6.35 cm. This structure definition was assumed uniform across the entire forebody and is described in Table 3. HT-424 is a commonly used TPS adhesive with flight heritage in human spaceflight dating from the Apollo entry systems to sample return missions such as Stardust. Below the .03 cm thick HT-424 adhesive, 2.1 lb/ft^3 aluminum honeycomb is sandwiched between 0.1 cm thin M55J graphite fiber facesheets. It is at the lowest element in the substructure where the heating is assumed to be adiabatic.

The second change in the entry problem formulation is the stack-up initial temperature. UOP science payload power requirements necessitate three radioisotope thermoelectric generators (RTG) which creates additional heating that is contained within the aeroshell. During interplanetary travel the heating is expelled through radiators in the cruise stage but after separation from the cruise stage on approach to Uranus, the RTGs thermal load may affect the performance of the TPS by warming the bondline and other stack-up components. Simulations used the previous

stack-up initial temperature of -10°C but also explored the impact of a 30°C starting temperature to understand the TPS sizing sensitivity.

Material Selection	Material Thickness [cm]
HT-424	0.030
M55J composite	0.1
Al-hc-2.1-2.5in	6.35
M55J composite	0.1

Table 3 Forebody substructure definition and thickness.

B. TPS Sizing Results

The HT-424 adhesive is rated for short-term operations up to 250°C, and this temperature constraint serves as the maximum limit for TPS system sizing. The freestream temperature, which averages to -10°C over the trajectory (consistent with previous analysis), is another input to TPS sizing. With the discussed trajectory environments, material stack-up, and starting temperatures, we can frame the entry problem and begin optimizing the TPS sizing for two initial temperature cases: -10°C and 30°C. Sizing was performed with NASA's Fully Implicit Ablation and Thermal response program (FIAT), which calculates the transient one-dimensional thermal response and surface thermochemistry of TPS stack-ups for design optimization[12]. The TPS thickness, not accounting for any environmental or material uncertainties, are shown in Table 4.

C-PICA Nominal Branch Solutions				
[cm]	T_0 = -10°C		T_0 = 30°C	
BP	Lift-Down	Lift-Up	Lift-Down	Lift-Up
0	3.35	3.02	3.49	3.15
10	2.84	2.55	2.96	3.05
20	2.68	2.40	2.79	3.03
30	2.59	2.32	2.71	2.42
40	2.75	2.46	2.86	2.57
160	3.28	2.96	3.42	3.09
170	2.99	2.69	3.12	2.81
180	3.00	2.70	3.13	2.81
190	3.17	2.86	3.31	2.98

Table 4 Nominal TPS thickness for C-PICA for both trajectories on select forebody body points and each starting temperature.

Table 4 shows the C-PICA thicknesses at each body point, for each trajectory, and for each initial temperature assumption. The trends of required thickness at each body point are consistent across all trajectories, with the leeward body points (BP10 to BP40) requiring the least amount of insulation and the stagnation point (BP0) and windward shoulder (BP160) necessitating the most. This aligns with the applied heat loads depicted in Table 2.

In the nominal branch sizing, a subset of body points on both sides of BP0 and BP160 was analyzed to confirm the worst-case body (driving body point) locations were included. The results of the Lift-Down thickness analysis are compared to those of the Lift-Up trajectory, with Lift-Down requiring more insulation than predicted from the heat load table.

The influence of initial temperature was as expected, with thickness growth observed for the warmer starting temperature. In the nominal branch, the additional Thermal Protection System (TPS) necessary for warmer starts was found to be approximately 4%. At higher initial temperatures, the surface energy re-balancing and convective heating into the TPS is lowered as well as conduction toward the bondline. While the influence is as expected, the magnitude is low, indicating that the C-PICA sizing and mass is not strongly influenced by the initial temperature of the heat shield.

The process for determining TPS sizing margins rely on Monte Carlo simulations, and assumptions about variability of key ablator attributes within the FIAT model. Monte Carlo analysis was performed using the MCFIAT tool, which is based on FIAT, to evaluate the initial temperature systems at the two most stressing body points from the nominal

branch solutions (BP0 and BP160). The analysis tracks peak bondline temperatures while distributing stack-up material properties, which are informed by Gaussian 2σ uncertainties. The 99.97% bounding peak bondline temperature was compared to the average peak bondline temperature across all Monte Carlo runs to determine a thermal margin, which informs the third branch of sizing in the RSS process. The C-PICA material property $2\sigma/\mu$ uncertainties were adopted from the Mars2020 project, which used an older version of PICA-D. These representative uncertainties were applied to both virgin and char TPS terms, including density, specific heat, conductivity, and emissivity. Each substrate material system received uncertainties for similar virgin properties, with a few additional terms perturbed in the TPS, including decomposition parameters, blowing reduction, and pyrolysis gas enthalpy. The uncertainties are presented in Table 5.

TPS Parameter	$\frac{2\sigma}{\mu}$ **Uncertainty**	**Substrate Parameter**	$\frac{2\sigma}{\mu}$ **Uncertainty**
TPS Virgin State		*Adhesive*	
Density	5	Density	10
Specific Heat	5	Specific Heat	10
Conductivity	20	Conductivity	20
Emissivity	5	Thickness	25
TPS Char State		*Honeycomb*	
Density	same as Virgin	Density	5
Specific Heat	10	Specific Heat	10
Conductivity	same as Virgin	Conductivity	25
Emissivity	5	Thickness	5
Other		*Facesheet*	
Decomposition Parameter	20	Density	10
Blowing Reduction	20	Specific Heat	10
Pyrolysis Gas Enthalpy	25	Conductivity	25
		Thickness	10

Table 5 Percent uncertainty in material modeling parameters for Monte Carlo simulations.

The resultant thermal margins from four Monte Carlo simulations with 10,000 runs each are shown in Table6. These margins are used as a knockdown in the bondline temperature constraint to size the material property uncertainty branch. The Monte Carlo analysis generally converged within 2,000 runs and the TPS thermal conductivity, both virgin and char, were the most correlated properties to the peak bondline temperature.

Finally, incorporating each of the three branches, the results of the RSS thicknesses are presented in Table 7. Observed trends follow those discussed from the nominal branch. The thickest solution is for the nose point BP0 in the Lift-Down trajectory and the warmer starting temperature of $30°C$. As was observed in the nominal branch, the TPS thickness sensitivity to initial temperature is about a 4% growth in a $40°C$ warmer starting temperature. The original initial temperature of -10$°C$ has a final margined thickness of 4.96 cm assuming a constant thickness TPS, yielding an approximately 250 kg heatshield. Based on these solutions, there may be an option to trim TPS material from the leeside of the vehicle to save mass, however, the CFD solutions used to generate the sizing environments are laminar and notably, integrating turbulent solutions into the analysis reveals that the leeward thickness required approaches the thickness required on the windward side. Ultimately, the evolution of the trajectory and vehicle structure has reduced the forebody TPS mass compared to the previous paper where C-PICA needed 5.22 cm. However, considering the impact of the RTGs may return the solution to nearly the same thickness, 5.17 cm.

Initial Temperature	**Nose BP0**	**Flank BP160**
-10°	72.55°	73.12°
30°	64.35°	66.02°

Table 6 Resultant thermal margin for forebody TPS from MCFIAT simulations of two body points at two initial temperatures.

C-PICA Margined Solutions					
[cm]		T_0 = -10°C		T_0 = 30°C	
Geometry	BP	Lift Down	Lift Up	Lift Down	Lift Up
Nose	0	4.96	4.49	5.17	4.68
LeeSide	10	4.24	3.82	4.44	3.99
	20	4.03	3.62	4.04	3.62
	30	3.90	3.51	4.09	3.68
	40	4.12	3.70	4.30	3.87
WindSide	160	4.85	4.38	5.06	4.57
	170	4.46	4.01	4.65	4.19
	180	4.46	4.02	4.66	4.21
	190	4.70	4.24	4.90	4.43

Table 7 RSS-sized TPS thickness for C-PICA for each trajectory on all forebody body points and both initial temperatures.

V. Mission Trade Study and Sensitivities

The baseline concept in DAC5 is similar to that of DAC3. However, two more radical concept alterations were studied in this work. The impact on the C-PICA TPS was evaluated in two such trade studies, the first is a separation trade and the second an entry velocity trade.

A. Heatshield Separation Trade Study

The separation timing of the aeroshell from the delivered orbiter is a critical consideration. After the aeroshell has survived the heat pulse associated with atmospheric entry, the heat load continues to affect the material, causing a process known as "soak back." In this regime, the surface cools radiatively but continues to conduct energy to the bondline and vehicle. The longer the heatshield remains attached to the vehicle, the more thermal protection system (TPS) material is required to insulate the bondline. An illustration of the aerocapture operational sequence is presented in Fig.5. Key locations on the sequence include the rarefied atmosphere with low aeroheating conditions (point 5), the exit from this region (point 6), and the separation of the heatshield (point 8). The baseline scenario assumes separation 10 minutes after exit from the rarefied atmosphere, resulting in a C-PICA TPS thickness of 4.96 cm, with an associated starting temperature of -10°C. Two alternative separation times are explored: Scenario 2 separates 65 seconds after exit, providing one minute of egress margin for atmospheric modeling and 5 seconds for the vehicle to rotate 180° (point 7) and safely leave the heatshield behind. Scenario 3 considers separation at an altitude of 2500 km, when the aeroshell is within the rarefied atmosphere but after the guidance phase has ended at 1000 km (point 4). Analysis suggests that this altitude provides an equivalent atmospheric heating rate to the bondline heating rate from thermal soak back, serving as an best-case scenario for early heatshield separation [9].

C-PICA thickness RSS calculations for each scenario are as follows:

- Scenario 1: separation 600 seconds after rarefied atmospheric exit. 4.96 cm (~250 kg C-PICA heatshield)
- Scenario 2: separation 65 seconds after rarefied atmospheric exit. 4.75 cm (~96% thickness)
- Scenario 3: separation at 2500 km (1120 seconds) within rarefied atmosphere. (~89% thickness)

The scale in reduction of C-PICA thickness can be better understood by studying Fig.6 in which nominal branch results are shown instead of the final margined sizing because the added TPS thickness and insulation for flight obscure heating indications at the bondline that inform the optimization process in the individual sizing branches. After peak heating, surface conduction becomes negative with a net energy loss to the system while the impact of peak heating is delayed by approximately 500 seconds before reaching the bondline. Once bondline conduction peaks it too reduces until thermal energy is pulled away from the bondline at roughly 1525 seconds. This is a critical transition because any additional time held onto the heatshield after this transition will not impact the sizing of the TPS. The limited reduction in TPS thickness moving from Scenario 1 to Scenario 2 is reasonable with this context. More thickness impact is found when moving from Scenario 2 to Scenario 3. By stepping further to the left in the bondline conduction trace, more heat load is removed and TPS can be thinned. Each of the three branches have different thickness sensitivity to the separation timings but the cumulative effects are represented above. In summary, approximately 10% of the TPS mass could be saved by separating within the rarefied atmosphere. However, the baseline approach keeps this extra 10% (25

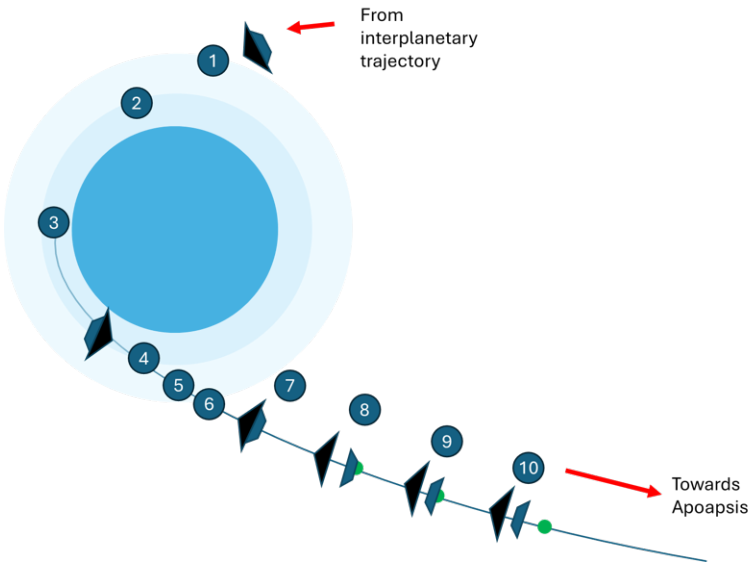

Fig. 5 Aerocapture Concept of Operations

kg of C-PICA) to maintain separation time flexibility; heatshield mass may also be needed for vehicle center-of-gravity reasons as well.

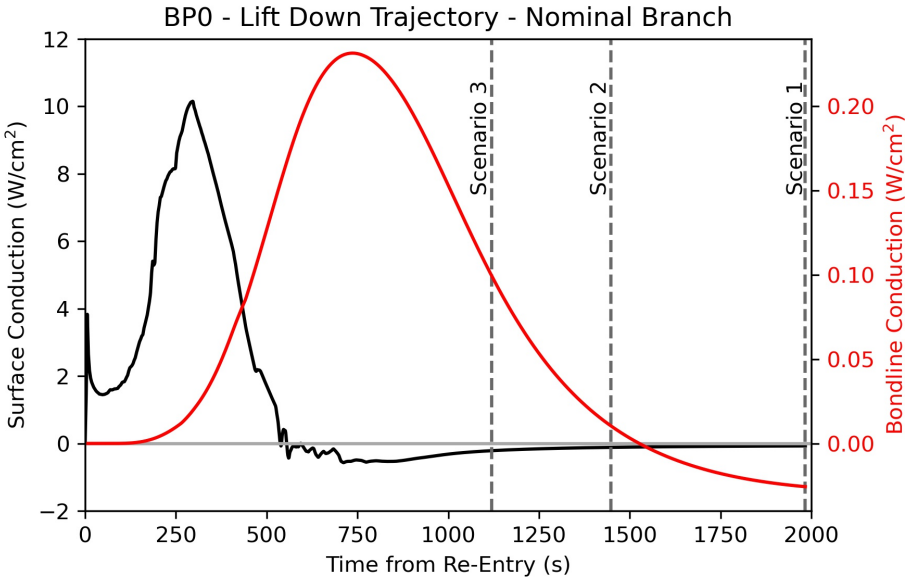

Fig. 6 Conduction traces at the C-PICA TPS surface and bondline for the nominal branch of the Lift Down Trajectory at the nose location (BP0). Vertical dashed lines indicate the time of separation for each of the three Con-Ops scenarios.

B. Entry Velocity Trade Study

An important objective of the project was to highlight the benefits of aerocapture at Uranus applying only existing technology. This led to using the Falcon Heavy Expendable as the launch vehicle with 2036-2038 launch dates that do not have access to Jupiter fly-bys. This baseline reaches Uranus with a V_∞ of 11.3 km/s. However, because a Uranus

flagship mission is likely to be designed and launched in the 2030's, launch vehicle capability may improve. For more information on launch vehicle assumptions and interplanetary trajectories see [13] where Space Launch System (SLS) and Starship based interplanetary trajectories are explored. One advantage of aerocapture for UOP over propulsive orbital capture is that aerocapture hardware becomes more efficient with increasing approach velocities, provided that the entry conditions remain within the capabilities of the TPS materials. A host of arrival velocities from 14 km/s to 22 km/s are explored for viability with a C-PICA heatshield.

With higher entry velocities the associated aerocapture trajectory environments are also increased. Despite the velocity increase, pressure and shear environments for the V_∞'s of 14-22 km/s remain less than half an atmosphere and 200 Pa, respectively. Neither of these conditions are stressing for C-PICA. Combined convective and radiative heat flux as well as total heat load are shown in Figure 7(a). Note, that heat loads from lift down trajectories are 20-35% larger with a maximum of 170 kJ/cm^2. Regarding, heating rates, the current arc-jet test limit of a tiled C-PICA and RTV-560 system is 600 W/cm^2. The V_∞ = 18 km/s Lift-Up trajectory reaches roughly 650 W/cm^2 and can be thought of as the current soft limit. Based on the similarity of C-PICA to the PICA-D material system, it is likely that future testing will show C-PICA's capability with RTV-560 gap-filler to beyond 600 W/cm^2 and possibly high enough to bound the 1200 W/cm^2 maximum presented in this analysis. However, At V_∞ = 20-22 km/s, heat flux is not the only concern and integrated heat load may be a driver. The heat loads are approximately doubled with radiation beginning to grow exponentially as exhibited in Figure 7 which breaks out the heat flux into its components. Qualifying TPS material becomes a more difficult task as heating increases. While testing in combined convective and radiative heating environments is possible using NASA's Laser Enhanced Arcjet Facility (LEAF), there are limits to the heat flux that can be achieved[14]. Instead, a combination of combined and convective-only heating at environments beyond 600 W/cm^2 environments may be used in piece-wise fashion to qualify the material for the expected environment.

Taking these environments and returning to FIAT TPS analysis, nominal branch solutions were completed and MCFIAT analysis then produced a thermal margin shown in Table 8. The largest thermal margin, 95.7°C, was applied in each case for simplicity and means that the lower V_∞ cases have more conservatism built-in. The final C-PICA thickness for the driving body points of the nose point and windside flank are also presented in Table 8. The massive increase in heat load is not matched by the relatively minor increase in C-PICA thickness. This is due to the ablator response. At V_∞ of 11.3 or even 14 km/s, C-PICA is operating in a recessionless regime due to the inert composition of the Uranian atmosphere. This is the least efficient manner to operate an ablator like C-PICA. However, as heating rates rise so does the surface temperature. These higher surface temperatures paired with low surface pressures enable carbon sublimation to occur which transitions the TPS into the most efficient mode of energy rejection. In Table 8, the amount of recession shows the engagement of sublimation. With the higher surface temperatures re-radiation increases as well although this plays a lesser role in energy rejection. At 14 km/s re-radiation rates peak at 290 W/cm^2 while at 22 km/s the peak re-radiation rates are approximately 475 W/cm^2.

V_∞ [km/s]	**Thermal Margin** [°C]	**Nose BP0 [cm]**	**Flank BP160 [cm]**	**Stag Pt Recession** [cm]
14	79.2	5.53	5.24	0
16	84.3	5.63	5.35	0
18	88.5	5.75	5.4	0.1
20	92.7	5.88	5.58	0.2
22	95.7	6.05	5.7	0.35

Table 8 V_∞ Trade Results. MCFIAT Thermal Margin, Nose and Flank Body Point RSS Sizing, and Stagnation Point Recession.

VI. Aftbody Thermal Protection Systems

As discussed in the previous paper, the spacecraft's backshell geometry is shaped with two primary considerations: 1) to house the large antenna necessary for orbiter communications in deep space and 2) to prevent shock impingement and flow attachment on the aftbody. Updates to the backshell design are reported in the work of Gomez Del Rio [6]. The largest impacts on the geometry and environments are from a reduction in overall vehicle diameter, 5m to 4.57m, atmospheric model updates, and a new nominal trajectory which incorporates other changes to the overall mission. Environments for select body points are shown in Fig. 8. Note that windward shoulder body points are excluded from these plots and are generally treated separately from the rest of the aftbody discussion. Rapid growth in heating at the shoulder region is shown in Fig. 9. TPS treatment for this region are portrayed as schemes, with the heritage scheme utilizing flight-proven TPS implemented in a manner similar to Mars2020. The tailored and simplified scheme are

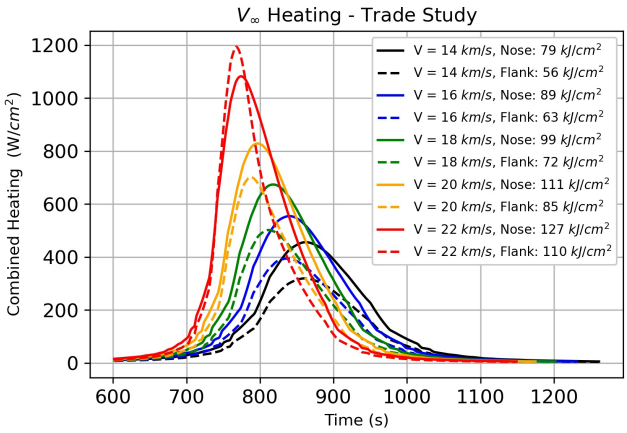

(a) Total Heating

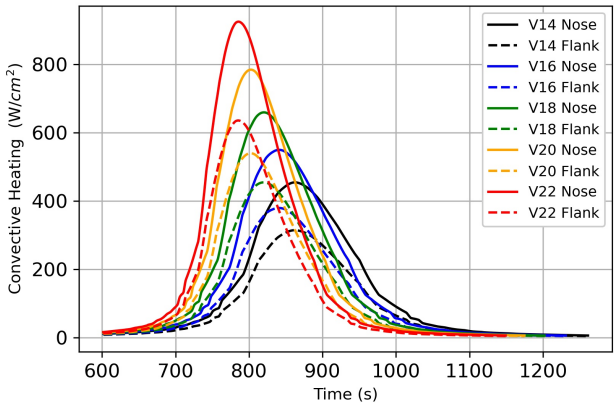

(b) Convective Heating

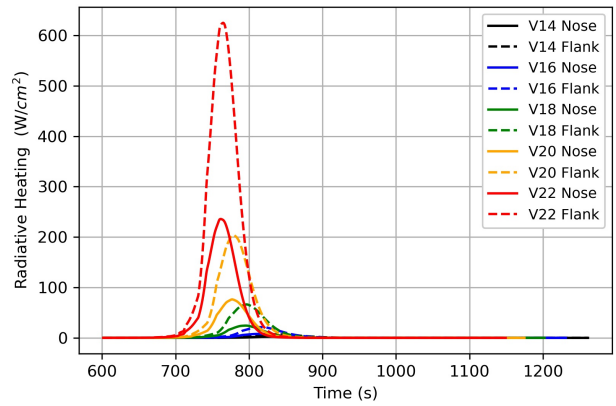

(c) Radiative Heating

Fig. 7 a) Total heating, b) convective heating, and c) radiative heating predictions for the forebody TPS across a range of V_∞ from 14 km/s to 22 km/s

successive departures from the heritage scheme with larger coverage by low-density TPS that does not have the same flight heritage or implementation. Each scheme implementation is visualized using a layout of the aeroshell aftbody that is defined with Lift-Up heating for reference in Fig. 10. As observed with the forebody environments, the peak aftbody environments are reduced compared to previous analysis. Aerothermal impacts due to reaction control systems (RCS) thrusters are not considered. The aftbody analysis that follows assumes an initial temperature of the system of 30°C to account for heat rejection from the RTGs.

A. Candidate Systems

The environments for the backshell are more than an order of magnitude lower in heating and pressure than the forebody environments, which allows for a broad consideration of TPS materials and implementation approaches to meet the aftbody design needs. Previously candidate systems covered heritage aftbody materials such as SLA-561V, Acusil II, and SIRCA-15. While each of these material systems are viable solutions, the benign conditions means that more mass efficient solutions likely exist. SLA-561V and Acusil II solutions were updated to the new geometry and environments while Felt Reusable Surface Insulation (FRSI) was also sized to explore alternate solutions. FRSI is a vaible alternate as a low-density TPS as it covered large portion of the Space Shuttle and has been tested to relevant environments[15]. Additionally, Spray-On Foam Insulation (SOFI) developed to protect launch vehicles like the SLS has been evaluated qualitatively for suitability. While foam-style TPS are not typical for applications of aeroshell TPS, they withstand environments similar to those presented here and represent an alternate approach that can save installation time and mass[16].

Material Selection	Material Thickness [cm]
RTV-560	0.010
M55J composite	0.02
Al-hc-4.3	1.91
M55J composite	0.02

Table 9 Aftbody substructure definition and material thickness.

B. TPS Sizing Results

SOFI is developed and sized by Marshall Space Flight Center. While detailed sizing information is not yet available, the material can be scaled to any desired thickness, is suited for cryogenic environments and a range of heating environments that the SLS may experience as part of the launch environment. It has been tested to heating environments in excess of 15 W/cm^2[17]. FIAT was used for SLA-561V, Acusil II, and FRSI thickness sizing and the process began with nominal branch sizing as seen in Table 10. The same thickness trends are observed in all three materials which follow the trends of heating environments, more heating requires more thickness to insulate the bondline. The majority of leeside body points did not meet the bondline temperature constraint even when using the minimum manufacturable thickness for the TPS. This is also the case for BP100. Rapid growth in required thickness occurs from BP150 to BP156. BP155 and BP156 are carried forward in this analysis, however an optimal design discussed in Subsection VI.C involves wrapping the forebody TPS around the shoulder eliminating the need for thicker aftbody solutions.

The environment for the thickest, non-shoulder body point, BP150, was used for the MCFIAT analysis. Uncertainty inputs for each TPS material is provided in Table 11. All substructure materials carried the same uncertainty as the forebody. The resulting thermal margin from MCFIAT analysis performed is shown in Table 12.

RSS thickness analysis resulted in a final sized thickness according to each body point as shown in Table 13. Acusil II as a system requires about three times the thickness as FRSI and SLA. As was seen in the nominal branch sizing, thickness quickly increase with the shoulder body points. Through evaluating the candidate TPS material's areal density, see Table 14,the mass efficiency can be understood. Acusil II provides RF transparency but at a significant mass cost of nearly 10 (kg/m^2). The mass of SLA-561V is much reduced at a little over 3 (kg/m^2) but given the extensive backshell area of almost 25 m^2, the backshell TPS alone would weigh 80 kg despite the low environments. Realistically, tailoring the TPS thickness depending on sizing requirements would reduce this mass. However, assuming a constant thickness backshell, expanding the trade space to FRSI reduce the SLA-561V mass by a third while opting into an additional benefit of material availability.

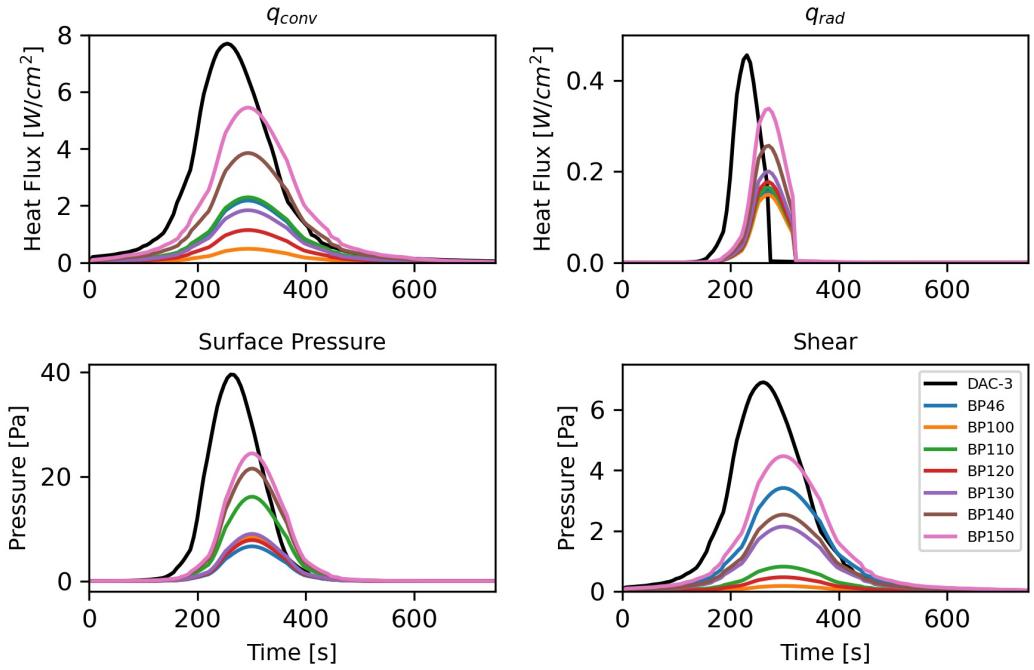

(a) Lift-Up environments

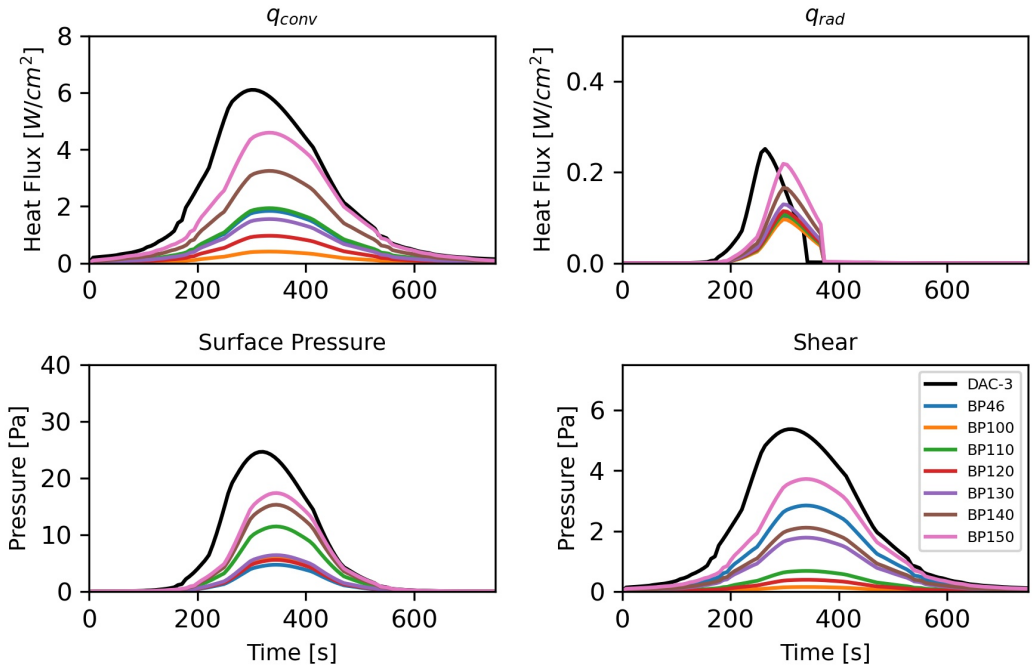

(b) Lift-Down environments

Fig. 8 Plot of a) Convective hot-wall heat flux (q_{conv}), b) radiative hot-wall heat flux (q_{rad}), c) surface normal pressure, d) shear stress for select body points on the aftbody.

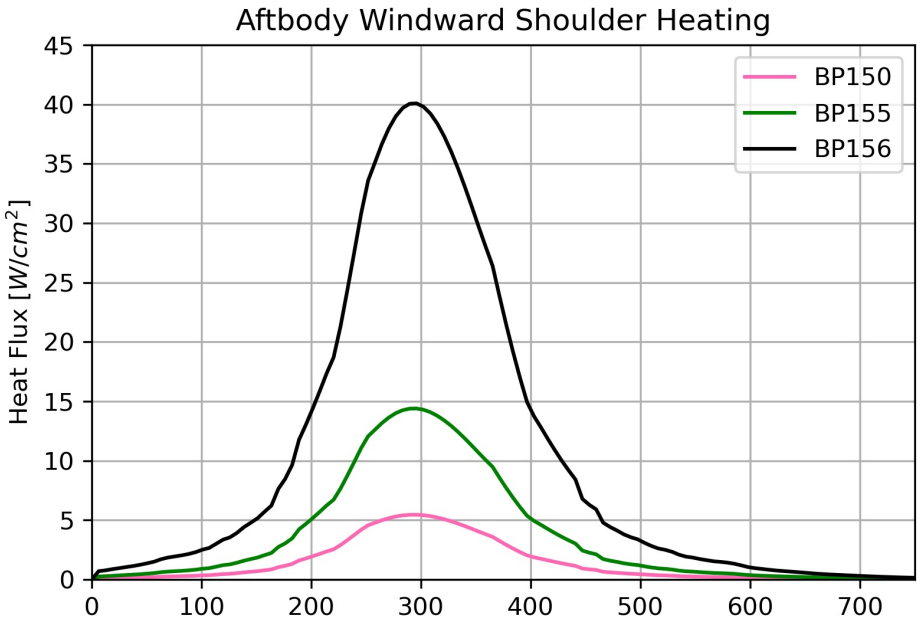

Fig. 9 Lift-Up total heating environments for shoulder regions on the aftbody.

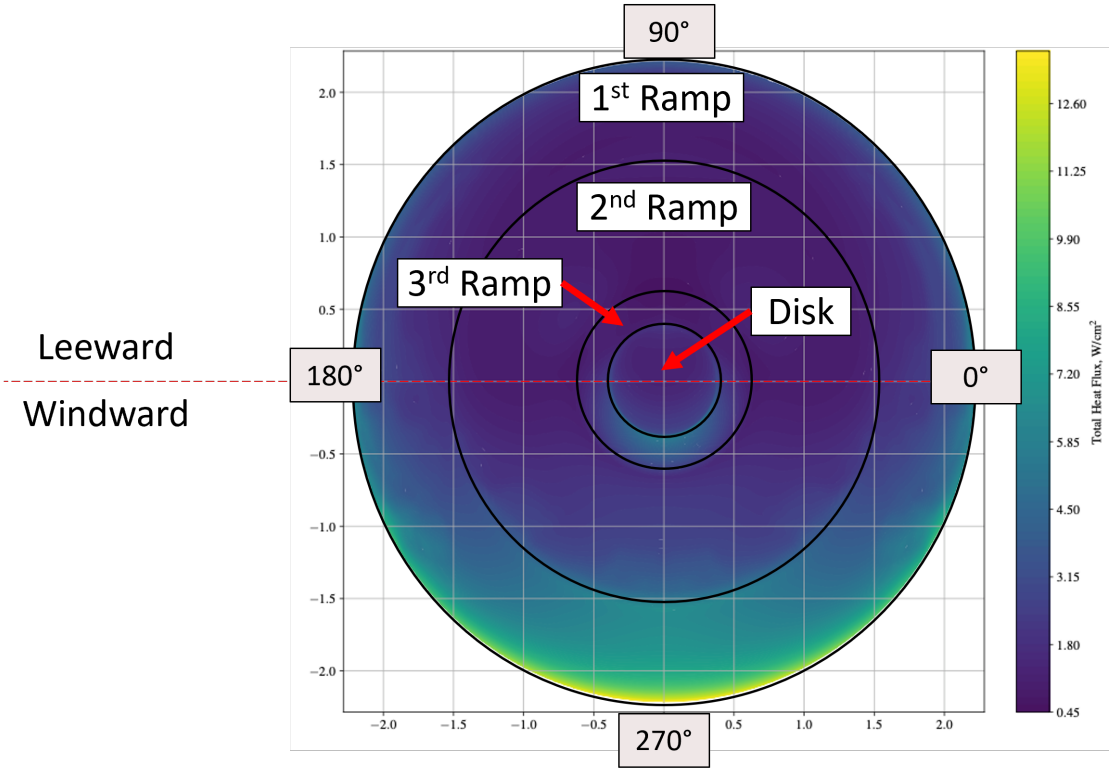

Fig. 10 Total heat flux distribution between the windwward and leeward portions of the aftbody for the Lift-Up trajectory with description for the ramp and disk features.

Aftbody Nominal Sizing (cm)			
BP	Acusil	FRSI	SLA
100	-	-	-
110	1.53	0.48	0.49
120	0.75	0.20	0.19
130	1.27	0.38	0.40
140	2.18	0.73	0.71
150	2.64	0.91	0.87
155	4.15	1.45	1.30
156	5.42	2.14	1.76
46	1.47	0.45	0.47
50	0.67	0.17	0.15

Table 10 Nominal TPS thickness for Aftbody Candidate TPS.

TPS Parameter	Acusil II	FRSI	SLA-561V
Virgin Density	10	6.5	6.5
Virgin Specific Heat	10	10	10
Virgin Conductivity	15	13	13
Virgin Emissivity	10	10	10
Char Density	Scaled with Virgin	Scaled with Virgin	Scaled with Virgin
Char Specific Heat	10	10	10
Char Conductivity	Scaled with Virgin	Scaled with Virgin	Scaled with Virgin
Char Emissivity	10	15	15

Table 11 Aftbody TPS $\frac{2\sigma}{\mu}$ uncertainty in material modeling parameters for Monte Carlo simulations.

Initial Temperature	Acusil II	SLA-561V	FRSI
30°C	50.97°C	33.93°C	39.42°C

Table 12 Resultant thermal margin from MCFIAT simulations at Body Point 150 assuming a warmed intial temperature.

ECI Aerocapture - DAC5 - Aftbody RSS Sizing			
BP	Acusil (cm)	FRSI (cm)	SLA (cm)
110	2.50	0.80	0.80
140	3.32	1.13	1.08
150	3.91	1.36	1.26
155	5.65	2.01	1.79
156	6.95	2.86	2.35
46	2.42	0.76	0.77
50	1.35	0.37	0.37

Table 13 RSS TPS thickness for Aftbody Candidate TPS.

Aftbody TPS	Acusil II	FRSI	SLA-561V
Areal Density kg/m^2	9.96	1.18	3.23

Table 14 Areal Density of the Aftbody TPS candidate materials according to BP150 sizing.

C. Application of Aftbody TPS

The application of TPS to an entry vehicle is often TPS specific, and many missions have included multiple types of TPS in across the backshell. Three different TPS schemes are introduced below through which the layout of TPS is explored along with advantages and disadvantages. Beyond simply optimizing for mass, implications in reducing aftbody TPS mass promotes a shift in the position of the center of gravity toward the nose of the vehicle, increasing the vehicle's attitude control. Alternatively, a reduction in aftbody TPS may result in reductions of ballast weight at the nose of the aeroshell, therefore become multiplicative mass savings.

1. Heritage Scheme

A heritage scheme of aftbody TPS would follow the example of MSL, Mars2020, and Dragonfly. This scheme employs SLA-561V from the shoulder until the first angle change in the backshell. Acusil II meets SLA-561V at this transition and covers the remaining backshell. Figure 11 shows a top down view looking at the aftbody with shaded regions representing TPS locations. The advantages of this scheme is that the TPS is well characterized for the aerocapture heat flux and pressure and Acusil II has radio frequency (RF) transparency allowing use of the large, orbiter antenna contained within the aeroshell. Additionally, processes for manufacturing a backshell of this design exist. On the other hand, this heritage scheme represents a maximum in mass due to the TPS not being optimized for the heating levels experienced within the aerocapture mission. This approach carry a combined, sized mass of 93.5 kg. While uncommon for forebody TPS, changing thickness of TPS across regions of the aftbody is common, so the challenges associated with implementation are assumed to be part of the existing knowledge set. The mass estimate is calculated by interpolating between body point thickness estimates from Table13 and rounding to the nearest 0.25 $inch$ interval for simplicity in manufacturing.

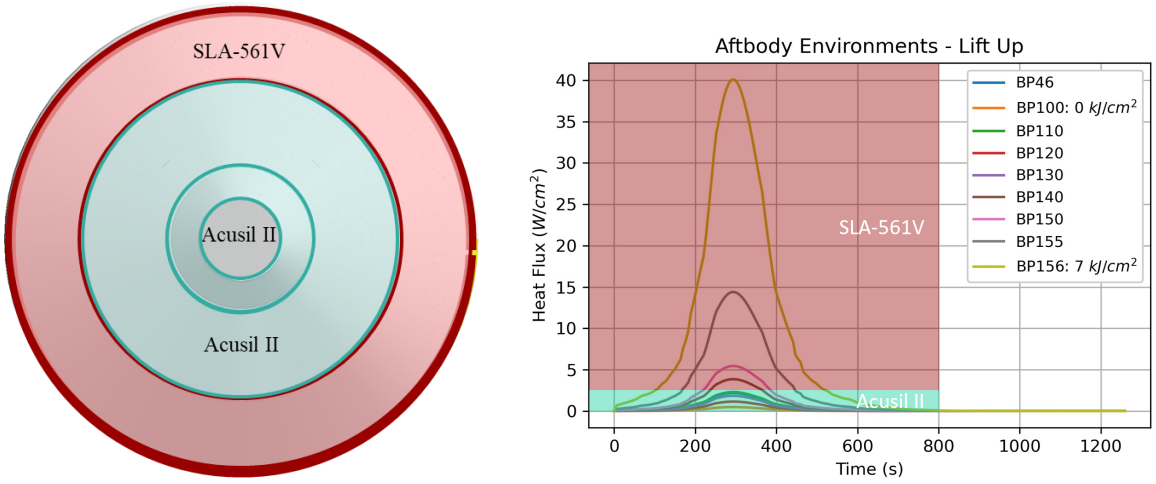

(a) TPS Layout

(b) Time history of heat flux across select body points color-coded by TPS solution employed.

Fig. 11 Heritage TPS Layout for aftbody utilizing SLA-561V on the 1st ramp with Acusil II on remaining surfaces for RF-transparency.

2. Tailored Scheme

An alternate layout that balances mass performance and preserves spacecraft communication operations is to engage C-PICA's conforming nature and bend the material around the shoulder of the forebody creating a small lip on the windward side of the aftbody. Implementing a very low density TPS for the relatively low heating region before transitioning to Acusil II, maintaining the RF-transparency for the antenna area. Figure 12 illustrates this layout. The very low density TPS could be SOFI or FRSI. The advantage of this scheme is a balance of mass savings while simplifying the TPS space to a single procurement. The disadvantage of this setup is that neither of the candidate TPS solutions have been used for this application and likely require additional testing and analysis. The tailored scheme uses both NASA and commercial TPS with variable thickness and has an estimated total mass of 67.9 kg.

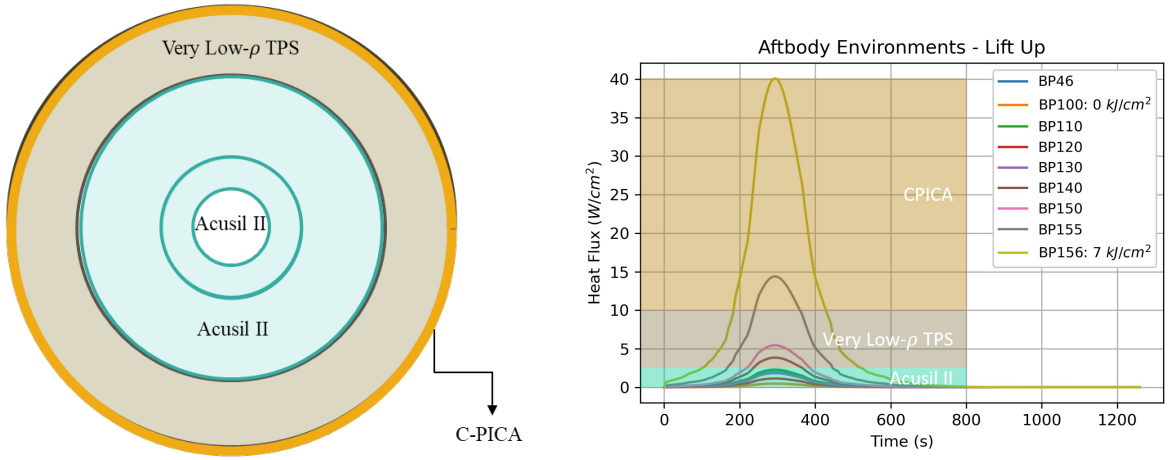

(a) TPS Layout

(b) Time history of heat flux across select body points color-coded by TPS solution employed.

Fig. 12 Tailored TPS layout utilizing C-PICA wrap-around shoulder, Very Low-ρ TPS on the 1st Ramp, and Acusil II for remaining surfaces.

3. Simplified Scheme

Finally, the simplified scheme uses as few TPS materials as possible to protect the vehicle from atmospheric re-entry environments. This layout, shown in Figure 13, keeps the C-PICA rim on the windward side but removes the heavy Acusil II and replaces it with continuous very low density TPS. This scheme carries significant mass savings at the back of the vehicle while simplifying the procurement and installation processes. FRSI was sized because it has detailed properties available in FIAT, and tailored sizing was performed across the ramps and disk. The total mass for this layout is 25 kg. Still, what remains uncertain is the efficacy of a low-density TPS like FRSI in RF-transparency and this must be evaluated.

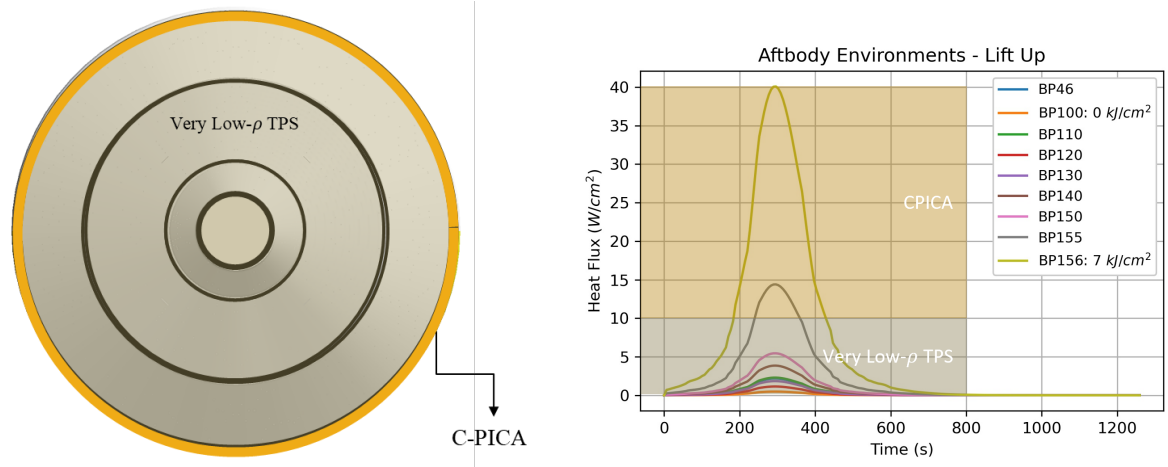

(a) TPS Layout

(b) Time history of heat flux across select body points color-coded by TPS solution employed.

Fig. 13 Simplified TPS Layout for aftbody utilizing C-PICA wrap-around shoulder and single Very Low-ρ TPS.

VII. Aeroshell Seal and Instrumentation Windows

Beyond the typical forebody and aftbody TPS, additional aeroshell components are subjected to the high-temperature environments and materials must be appropriately selected and sized to performance requirements.

A. Aftbody Interface Seals

As the aeroshell is a complex geometry, there are a variety of interfaces that require a seal to prohibit hot gas ingestion into the vehicle and the sensitive payload. The most critical interface exists at the interface of the forebody and aftbody. While additional seals exist, such as those around service doors and ports, this paper only assesses the main interface between the forebody and aftbody. This interface is estimated to be between body points BP 157 and 155, depending on the length of the C-PICA forebody shoulder wrap. Based on the heating level of approximately 40 W/cm^2, typical glass seals that have been employed in previous missions are acceptable, especially when considering the knock-down of heating from a seal that is recessed from the OML. While this is not expected to be a challenging aeroshell component, should the design require more benign environment, moving the seal location toward the aft-side of the vehicle by further extending the C-PICA wrap-around shoulder tiles would reduce the predicted heating.

B. Aftbody Instrumentation Windows

The aftbody is primarily designed for protecting the science payload during atmospheric entry and potentially also for allowing communications using the orbiter antennae. However, the aftbody is also the easiest place to install windows to allow for science and required navigation operations during the cruise stage of the mission. The windows must be sufficiently transparent to the desired wavelength for selected instrumentation, but critically must also be thermally stable throughout the atmospheric flight. Fortunately, many mission- relevant window material options have flight heritage. Listed in Table 15 are window material options, corresponding melt temperatures, and if applicable, heritage missions for the material as windows for science instruments. Non-mission threatening degradation of windows during atmospheric flight is acceptable, as the use as windows is intended during the cruise stage. Testing may be required to prove do-no-harm to the sensing elements as a result of signal passing through the windows during aerocapture maneuvers.

Wavelength Range	UV	Vis	IR	FIR
Window Material	UV Fused Silica	Fused Silica	Sapphire	Germanium
Transmission Range (μm)	0.18-2.1	0.18-2.1	0.2 - 5.0	0.1 - 20.0
Mission Heritage	Juno	New Horizons	New Horizons	Lunar Reconnaisance Orbiter

Table 15 Candidate Window materials for select instrument wavelengths, mission uses.

VIII. Development Needed for a Low-Risk TPS Solution on an Aerocapture Mission to Uranus

A. Forebody

C-PICA was chosen for the forebody based on the suitability for the predicted heat flux and pressure environments, coupled with the demonstrated performance in arc-jet testing and the manufacturability advantages over rigid PICA-D. While a gap-filler solution similar to Mars2020 and MSL has been shown in arc-jet testing, this solution may not be appropriate for a compliant system when fabricated and implemented on the full-scale vehicle. In addition, the unique H/He environment may necessitate a change in the gap-filler material and implementation. A trade on the gap-filler system for C-PICA at relevant scale vehicle should be performed to alleviate difficulties in implementation. In addition, arc-jet testing is needed for C-PICA and the gap-filler system in a relevant environment, at least in non-oxidizing gas to assess the material response, demonstrate performance at bounding conditions, investigate possible failure modes, and perform standard flight-lot acceptance testing. This is captured in Table16 as "Standard" in-line with typical arc-jet testing campaign performed for NASA missions. Beyond implementation, forming of a wrap-around shoulder should be developed and tested to understand any detriments to the system response and allow for mitigations prior to aeroshell fabrication.

B. Aftbody

Depending on the scheme selected for aftbody TPS, there are varying degrees of forward work. While the heritage scheme is already demonstrated in flight, tailored testing should be performed to understand unique response of TPS to a H/He environment, or at least in non-oxidizing environments. With changes to a heritage scheme, a material development and qualification campaign should be undertaken to show that there are no limits to the material performance in a relevant

environment. Demonstration of fabrication at scale should be undertaken, and an assessment of the RF-transparency are some of the tasks to demonstrate the material is suitable for use. As stated before, detailed testing will be needed to assess interactions with the RCS regions of the aftbody.

Location	Forebody	Aftbody			
TPS	Tiled C-PICA	SLA-561V	Acsuil II	FRSI	SOFI
Source	NASA	Lockheed Martin	Peraton	NASA	NASA
Installation	Machine & Bond	Hand-pack & Machine	Hand-pack & Machine	Bond	Spray & Machine
Aerothermal Testing	Standard	Standard	Standard	Development	Development
Additional Needs	Gap-Filler Assessment			RF-Transparency	RF-Transparency

Table 16 Summary of developmental needs in aeroshell TPS for Aerocapture to Uranus.

IX. Conclusions

Aerocapture may greatly improve a UOP mission by reducing the cruise time to the destination, saving propellent, allowing for launch flexibility and greater science payload. To perform aerocapture, the payload must be housed in an aeroshell that is protected from the entry environment. TPS sizing predictions have been shown based on refined analysis of an updated aerocapture vehicle to Uranus using the UOP payload. C-PICA still shows sufficient aerothermal performance and a manufacturable thickness of 5.17 cm for a vehicle arriving to Uranus with a velocity of 11.3 km/s. A sensitivity study of the heatshield separation found that earlier release of the heatshield does reduce necessary C-PICA mass by approximately 10% which could be used elsewhere in the system or retained for margin against heating increases. Results from varying vehicle arrival velocities to Uranus based on changes in interplanetary trajectories suggest that tiled C-PICA remains the appropriate forebody TPS up to an arrival velocity of 18 km/s, but additional qualification testing of the system is required to determine performance sensitivities as sublimation is activated at arrival velocities beyond 18 km/s. For the aftbody, updated sizing results were given for heritage TPS systems and alternate TPS materials were explored due to the less severe heating environment. While heritage systems are well suited for the predicted environments, mass-savings of between 26 and 68 kg are possible along with manufacturing simplification gained by direct bonding or using spray application. For all systems used, qualification campaigns should be performed in non-oxidizing environments to ensure that there are no issues with performance. In addition, manufacturing demonstrations should be undertaken to show viable implementation for the aftbody. Ultimately, a robust set of TPS exists now, and with continued development, efficient TPS options will be well positioned for future aerocapture missions to Uranus.

X. Acknowledgements

The authors would like to thank Ethiraj Venkatapathy and Matthew Gasch for discussion relating to TPS design and C-PICA implementation. Additionally, the authors would like to thank Elizabeth Schofield and Stephen Wess at MSFC for their continued support in assessing the viability of polymeric foam for the aftbody TPS design.

References

[1] National Academies of Sciences, E., and Medicine, *Origins, Worlds, and Life: A Decadal Strategy for Planetary Science and Astrobiology 2023-2032*, The National Academies Press, Washington, DC, 2022. https://doi.org/10.17226/26522, URL https://nap.nationalacademies.org/catalog/26522/origins-worlds-and-life-a-decadal-strategy-for-planetary-science.

[2] Lockwood, M. K., Edquist, K. T., Starr, B. R., Hollis, B. R., Hrinda, G. A., Bailey, R. W., Hall, J. L., Spilker, T. R., Noca, M. A., and O'Kongo, N., "Aerocapture systems analysis for a Neptune Mission," Tech. rep., 2006.

[3] Spilker, T. R., Adler, M., Arora, N., Beauchamp, P. M., Cutts, J. A., Munk, M. M., Powell, R. W., Braun, R. D., and Wercinski, P. F., "Qualitative Assessment of Aerocapture and Applications to Future Missions," *Journal of Spacecraft and Rockets*, Vol. 56, No. 2, 2019, pp. 536–545. https://doi.org/10.2514/1.A34056, URL https://doi.org/10.2514/1.A34056.

[4] Dutta, S., Shellabarger, E., Scoggins, J. B., Gomez-Delrio, A., Lugo, R., Deshmukh, R., Tackett, B., Williams, J., Johnson, B., Matz, D., Geiser, J., Morgan, J., Restrepo, R., and Mages, D., *Uranus Flagship-class Orbiter and Probe Using Aerocapture*, ???? https://doi.org/10.2514/6.2024-0714, URL https://arc.aiaa.org/doi/abs/10.2514/6.2024-0714.

[5] Morgan, J., Williams, J., Venkataphy, E., Gasch, M., Deshmukh, R., Shellabarger, E., Scoggins, J. B., Gomez-Delrio, A. J., Tackett, B., and Dutta, S., *Thermal Protection System Design of Aerocapture Systems for Uranus Orbiters*, ???? https://doi.org/10.2514/6.2024-0952, URL https://arc.aiaa.org/doi/abs/10.2514/6.2024-0952.

[6] Gomez-Delrio, A., Davis, W., Deshmukh, R., and Dutta, S., "Design Considerations for Aerocapture Delivery of Uranus Orbiter and Probe," *2025 AIAA SciTech Conference,* Orlando, FL, 2025.

[7] Deshmukh, R., Dutta, S., and Chadalavada, P., "6-DOF Uranus Aerocapture Trajectory Analysis," *2025 AIAA SciTech Conference,* Orlando, FL, 2025.

[8] Shellabarger, E., Scoggins, J., Hinkle, A., Deshmukh, R., Dutta, S., Agam, S., and Patel, M., "Aerodynamics of a Uranus Aerocapture System using a Mars-Heritage Entry Vehicle," *2025 AIAA SciTech Conference,* Orlando, FL, 2025.

[9] Scoggins, J., Hinkle, A., Agam, S., and Patel, M., "Forebody Aeroheating Environments for a Uranus Aerocapture System using a Mars-Heritage Entry Vehicle," *2025 AIAA SciTech Conference,* Orlando, FL, 2025.

[10] Milos, F. S., and Gasch, M., *Conformal Phenolic Impregnated Carbon Ablator (C-PICA) Arcjet Testing, Ablation and Thermal Response*, ???? https://doi.org/10.2514/6.2015-1448, URL https://arc.aiaa.org/doi/abs/10.2514/6.2015-1448.

[11] *VARDA Space Industries*, February, 2024. URL https://www.varda.com/platform/.

[12] Chen, Y.-K., and Milos, F. S., "Ablation and Thermal Response Program for Spacecraft Heatshield Analysis," *Journal of Spacecraft and Rockets*, Vol. 36, No. 3, 1999, pp. 475–483. https://doi.org/10.2514/2.3469.

[13] Mages, D., Restrepo, R., Chadalavada, P., Deshmukh, R., Dutta, S., and Benhacine, L., "Mission Design and Navigation for Uranus Aerocapture Leveraging Super Heavy-Lift Launch Vehicles," *2025 AIAA SciTech Conference,* Orlando, FL, 2025.

[14] Cushman, G., Alunni, A., Balboni, J., Zell, P., Hartman, J., and Empey, D., *The Laser Enhanced Arc-Jet Facility (LEAF-Lite): Simulating Convective and Radiative Heating with Arc-jets and Multiple 50-kW CW Lasers*, ???? https://doi.org/10.2514/6.2018-3273, URL https://arc.aiaa.org/doi/abs/10.2514/6.2018-3273.

[15] Milos, F. S., Scott, C. D., and Del Papa, S. V., "Arcjet Testing and Thermal Model Development for Multilayer Felt Reusable Surface Insulation," *Journal of Spacecraft and Rockets*, Vol. 51, No. 2, 2014, pp. 397–411. https://doi.org/10.2514/1.A32460, URL https://doi.org/10.2514/1.A32460.

[16] Kanner, H., Stuckey, C., and Davis, D., *Recession Curve Generation for Space Shuttle Solid Rocket Booster Thermal Protection System Coatings*, ???? https://doi.org/10.2514/6.2002-3334, URL https://arc.aiaa.org/doi/abs/10.2514/6.2002-3334.

[17] Schofield, E., private communication, September, 2024.